Physicochemical properties of steelmaking slags for the mitigation of CO_2 emissions in steel sector

M.J. Lee[1], J.H. Heo[2], J.H. Park[3,]*

1. Student, Department of Materials Science and Chemical Engineering, Hanyang University, Ansan, 15588, Korea.
2. Senior Researcher, Korea Institute of Geoscience and Mineral Resources (KIGAM), Daejeon, 34132, South Korea.
3. Professor, Department of Materials Science and Chemical Engineering, Hanyang University, Ansan, 15588, Korea. Email: basicity@hanyang.ac.kr

Keywords: CO_2 emissions; EAF; ESF; DRI; HBI; Phosphate capacity; Foaming; Viscosity

ABSTRACT

In the present paper, the challenging points regarding the high temperature physical chemistry of slags to achieve the improved and stable EAF or ESF technology on the way to green steel will be reviewed, and the recent experimental and modelling research will be discussed. For example, the initial melting phenomena of HBI and the slag formation behaviour was observed using a high-frequency induction furnace. Main component of gangue oxides in HBI was SiO_2, Al_2O_3, and CaO in conjunction with unreduced iron oxide. To increase the dephosphorization efficiency, the distribution ratio of phosphorus between metal and slag was calculated using FactSage software and was compared to the measured results. The optimization of slag chemistry is required not only for maximum dephosphorization efficiency with good slag foamability but also for minimum slag volume with less refractory corrosion in EAF process. The slag chemistry is also one of key parameters affecting the operation efficiency in ESF in view of FeO reduction behaviour, viscosity, sulphide capacity, etc.

INTRODUCTION

It is well known that global CO_2 emission from iron and steel sector is *ca*. 7%, which is approx. 1/3 of industrial energy use. Hence, many steel companies are trying to develop the electric arc furnace (EAF) and/or electric smelting furnace (ESF) steelmaking processes instead of blast furnace (BF) and basic oxygen furnace (BOF) integrated routes by employing high amounts of direct-reduced iron (DRI) and/or hot briquetted iron (HBI) to mitigate CO_2 emissions. The DRI/HBI as substitutes for virgin scrap in EAF has been used because DRI/HBI does not have tramp elements. Unfortunately, however, commercially available DRI contains the relatively high levels of phosphorus and gangue oxides, which adversely affects not only the steel properties but also the operation efficiency. Alternatively, integrated steel mills have focused on the ESF process by keeping conventional BOF to produce high-end quality products. The H_2-reduced DRI or HBI are able to be charged in ESF in conjunction with fluxes and carbon sources, producing hot metal and BF type slag. The high-grade iron ores (Fe>68%) are economically used in EAF, whereas low-grade iron ores (Fe<65%) are targeted to be used in ESF (Wimmer et al., 2023).

CHEMISTRY OF DIRECT-REDUCED IRON (DRI)

The composition distributions of gangue oxides including unreduced iron oxide in commercially produced DRI are shown in the CaO-SiO_2-FeO ternary phase diagram (FIG 1). Here, the oxide composition was normalized to ternary system by excluding metallic iron (M.Fe). So, the chemical compositions of oxide phases widely vary, i.e., 5 to 25% CaO, 10 to 30% SiO_2, and 60 to 80% FeO with minor amounts of MgO and Al_2O_3. By adding fluxing materials such as lime and dolomite, the EAF refining slag can be formed and be working in dephosphorization reaction after melt-down of the charged raw materials such as DRI, HBI and scrap.

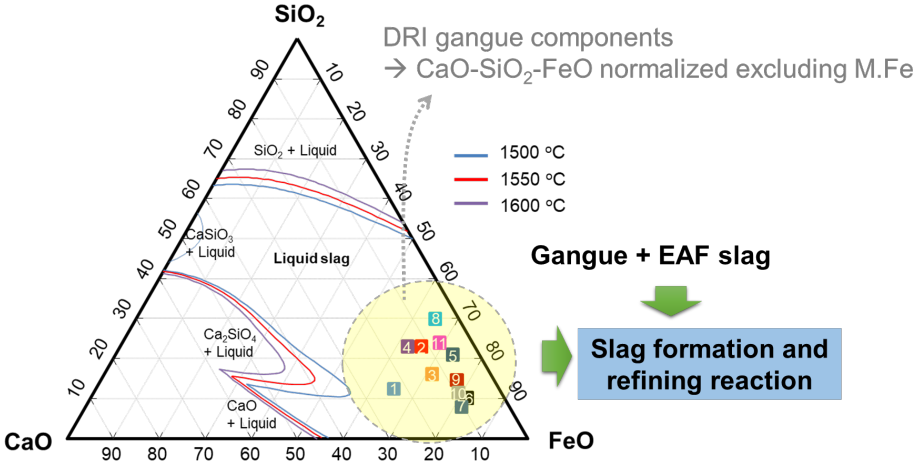

FIG 1 – Compositions of gangue oxides normalized into the CaO-SiO_2-FeO ternary phase diagram.

SLAG FORMATION DURING MELTING HOT BRIQUETTED IRON (HBI)

The reaction phenomena for the state of initial melting of HBI during heating are shown in FIG 2. Before melting, HBI samples were cut into small pieces and polished to characterize the gangue oxides and carbon distributions in HBI. A high-frequency induction furnace was used to observe the melting behavior and the slag-metal reactions. 400g HBI was charged in a fused magnesia crucible. The experimental temperature was increased by 10ºC/min rate and hold at 1550ºC. Partially melted iron briquette, FeO-SiO_2 (fayalite) based slag and CO gas evolutions were observed during initial melting. Here, CO gas originated from carbothermic reaction between FeO and carbon in HBI as given in Eq. [1].

$$FeO(s) + C(s) = Fe(l) + CO(g) \quad [1]$$

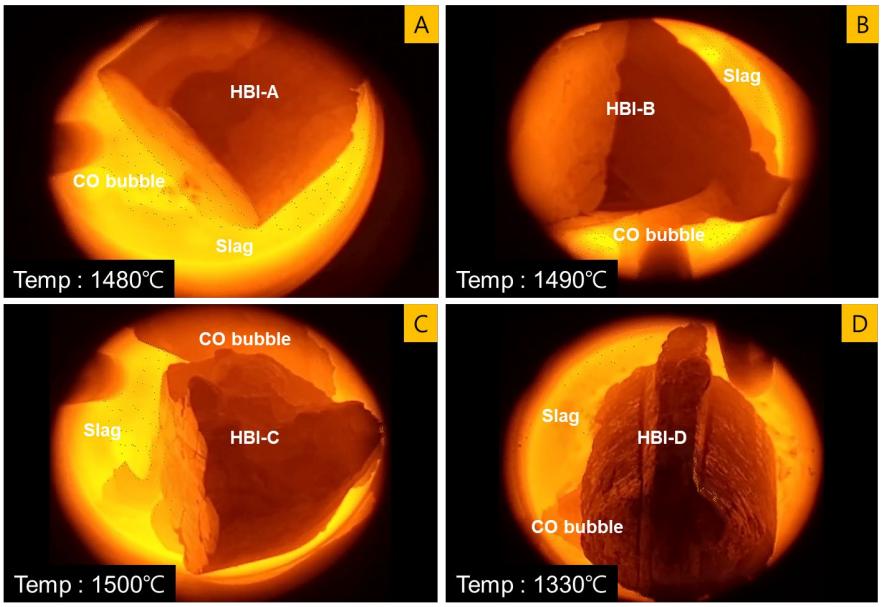

FIG 2 – Snapshot for initial melting of HBI with carbon content of (a) 1.3, (b) 1.0, (c) 1.4 and (d) 2.1 wt%.

In FIG 2, it is interesting that the melting initiation temperature decreases from about 1490(±10) ºC to 1330(±10) ºC by increasing the carbon content in HBI from about 1.2(±0.2) to 2.1(±0.1) wt%. It was reported that 1wt% carbon in DRI or HBI can potentially contribute to an increase of productivity (+0.8 to 1.5%) and iron yield (*ca*. +1%) as well as to a decrease of electrode consumption (-0.1 to 1.5 kg/t) and electric power (-15 to 25 kWh/t) in EAF operations (Sunyal, 2015; Hornby, 2021). Also, thin slag layer on the surface of molten steel was produced by the melting of gangue oxides in HBI and the absolute quantity of slag produced by gangue oxides in HBI increased with increasing HBI content. After melting, slag foaming was induced by CO gas evolution from the reaction between FeO in the molten slag with carbon in the molten steel. At this point, the changes in composition and amount of slag are strongly dependent on HBI content. Therefore, it is vital to evaluate the behavior of phosphorus in molten steel and slag according to HBI mixing ratio during specific reaction stages, such as melting and slag–metal reaction, to thermodynamically understand the dephosphorization reaction.

EFFECT OF DRI ON PHOSPHATE CAPACITY OF EAF SLAG

Phosphate capacity as a measure of the ability of a slag to absorb phosphorus can be defined as a function of temperature, basicity, and the stability of phosphate ion in the slag as follows (Wagner, 1975).

$$\frac{1}{2}P_2(g) + \frac{3}{2}(O^{2-}) + \frac{5}{4}O_2(g) = (PO_4^{3-}) \quad [2]$$

$$C_{PO_4^{3-}} = \frac{K_{[2]} \cdot a_{O^{2-}}^{3/2}}{f_{PO_4^{3-}}} = \frac{(\%PO_4^{3-})}{p_{P_2}^{1/2} \cdot p_{O_2}^{4/5}} \quad [3]$$

where $K_{[2]}$ is the equilibrium constant of Eq. [2], $a_{O^{2-}}$ is the activity of free O^{2-} ion, $f_{PO_4^{3-}}$ is the activity coefficient of phosphate ion in slag, and p_i is the partial pressure of the gaseous component i. Slag composition is expected to change with DRI content because gangue oxides in DRI dissolve into the slag. In particular, because SiO_2 content in DRI as a gangue oxide is relatively high (~5 wt%), slag basicity, which is the driving force of dephosphorization reaction based on Eq. [2], will decrease. Thus, it is vital to confirm the relationship between modified basicity index, e.g. $\log\{(X_{BO(=CaO+Na_2O+BaO+MnO)}/X_{AO(=SiO_2+B_2O_3)}\}$ and phosphate capacity, $\log C_{PO_4^{3-}}$, as shown in FIG 3(a) (Heo and Park, 2018). Phosphate capacity, $\log C_{PO_4^{3-}}$ clearly decreased with decreasing basicity and with increasing DRI content, indicating that a higher content of DRI unambiguously reduced dephosphorization efficiency by contributing SiO_2.

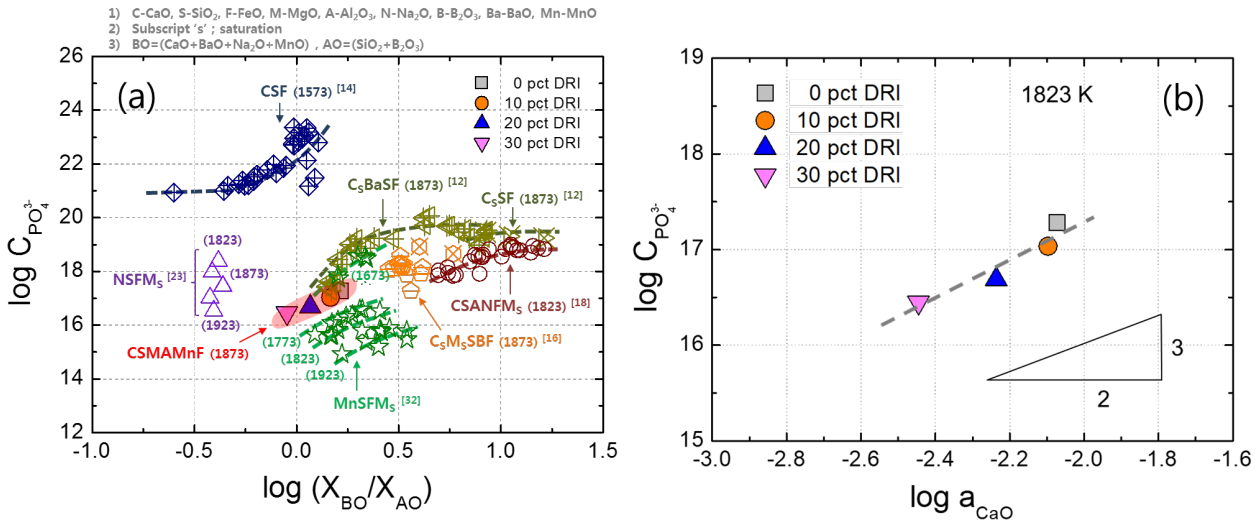

FIG 3 – Phosphate capacity, $\log C_{PO_4^{3-}}$ as a function of (a) modified basicity index, $\log(X_{BO}/X_{AO})$ for the FeO-bearing slags and (b) $\log a_{CaO}$ for the CaO-SiO_2-FeO-MgO-Al_2O_2-MnO slag.

Activity of CaO decreases and that of SiO_2 increases with increasing DRI content. CaO is known to behave as a representative basic component by contributing free oxygen ions (O^{2-}) in the slag as outlined in the following reaction (Sano, 1997).

$$(CaO) = (Ca^{2+}) + (O^{2-}) \quad [4]$$

$$a_{O^{2-}} = \frac{K_{[4]} \cdot a_{CaO}}{a_{Ca^{2+}}} \quad [5]$$

By combining Eqs. [3] and [5], the correlation between CaO activity and phosphate capacity can be deduced as follows:

$$\log C_{PO_4^{3-}} = \frac{3}{2}\log a_{CaO} - \frac{3}{2}\log a_{Ca^{2+}} - \log f_{PO_4^{3-}} + \text{Const.} \quad [6]$$

Based on Eq. [6], the phosphate capacity and activity of CaO are expected to exhibit a linear relationship with a slope of 1.5 on a logarithmic scale assuming that the composition dependencies of $a_{Ca^{2+}}$ and $f_{PO_4^{3-}}$ are not critical at a given temperature. Here, the activity of CaO was calculated from FactSage™(8.2) software with FTOXID and FACTPS databases. FIG 3(b) shows the linear relationship between phosphate capacity and the activity of CaO obtained using least square regression (Heo and Park, 2018). Hence, the activity of CaO can be used as a useful index representing the basicity of slag based on the linear relationship between phosphate capacity and the activity of CaO. It is noteworthy that the phosphate capacity of slag is strongly affected by the activities of CaO and SiO_2 in the slag.

CONTROL OF PHASE EQUILIBRIA FOR GOOD FOAMABILITY OF EAF SLAG

Slag foaming is strongly affected by the slag viscosity, which is dependent on the MgO content as well as basicity. The (Mg,Fe)O monoxide (magnesiowüstite, MW) and Ca_2SiO_4 (dicalcium silicate, C_2S) compounds suspended slags are frequently occurred in commercial EAF plant operation due to the heterogeneous slag composition, temperature fluctuations, and impurities in the fluxing agents. The solid+liquid multiphase slag affects the foamability and dephosphorization efficiency. For slag composition beyond the MW saturation limit, it is expected that slag viscosity is relatively higher than fully liquid slag due to precipitation of solid compounds according to Einstein-Roscoe equation (Roscoe, 1952; Heo and Park, 2021). A higher viscosity increases the foaming index (Σ), which is equal to the retention or traveling time of gas in the slag, which can be used as a quantitative index of foam stability (Ito and Fruehan, 1989). Hence, it is required to evaluate the effect of basicity on the foaming index. In the present study, the empirical equation of the foaming index of a multicomponent slag system was suggested by considering the thermophysical properties of slags as follows:

$$\Sigma = k\frac{\eta}{\sqrt{\rho \cdot \sigma}} \qquad [7]$$

where k, η, ρ, and σ are a constant, viscosity [Pa·s], density [kg/m^{-3}], and surface tension [N/m], respectively. The constant k was assigned a value of 999 due to the value obtained from a similar slag composition by Kim et al. (2001) The viscosity can be obtained by FactSage^{TM} software. Here, the effect of solid precipitation on slag viscosity is considered by using the Einstein-Roscoe equation. In addition, the density and surface tension are estimated using the polynomial expression by considering pure components, which are functions of temperature. Temperature dependencies of surface tension and density of slag components are available elsewhere (Heo and Park, 2019).

The foaming index of the FeO-bearing slags are compared in FIG 4 including Fruehan et al.'s (Ito and Fruehan, 1989; Jiang and Fruehan, 1991) data (Heo and Park, 2021). The foaming index of the $CaO\text{-}SiO_2\text{-}FeO\text{-}Al_2O_3\text{-}MgO\text{-}MnO$ system EAF slag and Fruehan et al.'s data generally decreases with increasing basicity up to C/S=1.0–1.2, depending on the slag composition, and it rebounds with increasing basicity, which is in excess of the liquidus composition. This behavior is strongly affected by the slag viscosity based on Eq. [7]. For slag basicity, C/S<1.2, the viscosity decreases with increasing basicity but beyond 1.2, the viscosity that apparently increases with increasing basicity is affected by the precipitation of solid compounds, contributing to increase the foam stability.

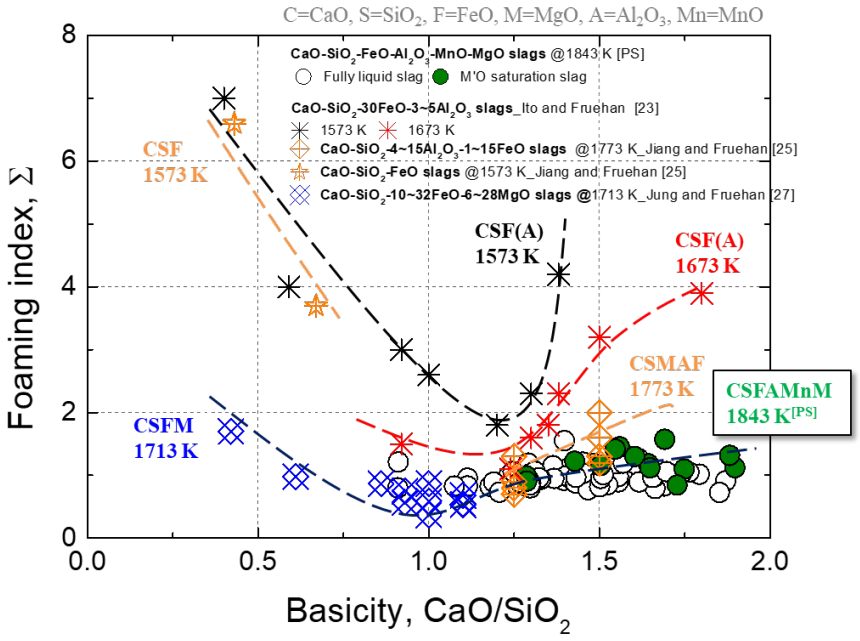

FIG 4 – Effect of CaO/SiO_2 ratio of slag and temperature on the foaming index (Σ) of FeO-bearing EAF slags.

CONCLUSIONS

The active use of H_2-reduced DRI and/or HBI has been widely increasing to mitigate the CO_2 emissions in steel sector. The contents of unreduced FeO (i.e., metallization degree) as well as gangue oxides such as SiO_2, Al_2O_3, etc. are significant factor affecting the electric furnace operations efficiency including FeO reduction, carburization, melting rate of DRI/HBI, dephosphorization, slag foaming, refractory corrosion, etc. These phenomena are expected to be quite different from conventional experiences using NG-reduced DRI/HBI in conjunction with virgin scrap. Consequently, the physicochemical properties of molten slags and fluxes should be further investigated by combining the experimental methodologies and computational modeling.

REFERENCES

Heo, J.H., Park, J.H. 2018. Effect of direct reduced iron (DRI) on dephosphorization of molten steel by electric arc furnace slag, Metall. Mater. Trans. B, vol. 49B, pp. 3381–3389.

Heo, J.H., Park, J.H. 2019. Assessment of physicochemical properties of electrical arc furnace slag and their effects on foamability, Metall. Mater. Trans. B, vol. 50B, pp. 2959–2968.

Heo, J.H., Park, J.H. 2021. Effect of slag composition on dephosphorization and foamability in the electric arc furnace steelmaking process: Improvement of plant operation, Metall. Mater. Trans. B, vol. 52B, pp. 3613–3623.

Hornby, S. 2021. Hydrogen based DRI EAF steelmaking – Fact or fiction? Proceeding of AISTech2021, Nashville, TN.

Ito, K., Fruehan, R.J. 1989. Study on the foaming of CaO-SiO_2-FeO slags, Metall. Trans. B, vol. 20B, pp. 509–521.

Jiang, R., Fruehan, R.J. 1991. Slag foaming in bath smelting, Metall. Trans. B, vol. 22B, pp. 481–489.

Kim, H.S., Min, D.J., Park, J.H. 2001. Foaming behavior of CaO-SiO_2-FeO-MgO_{satd}-X (X=Al_2O_3, MnO, P_2O_5, and CaF_2) slags at high temperatures, ISIJ Int., vol. 41, pp. 317–324.

Sano, N. 1997. Advanced Physical Chemistry for Process Metallurgy, Academic Press, New York, NY.

Sunyal, S. 2015. The value of DRI – Using the product for optimum steelmaking, Direct from Midrex, 1Q 2015.

Wagner, C. 1975. The concept of the basicity of slags, Metall. Trans. B, vol. 6B, pp. 405–409.

Wimmer, G., Rosner, J., Voraberger, B. 2023. Smelter for processing of low grade DRI, Proceeding of 6th ESTAD 2023, Düsseldorf, Germany.